Concurrent planar multiharmonic dual-band load coupling network for switching-mode power amplifiers

Danish Kalim and Renato Negra

Mixed-Signal CMOS Circuits, UMIC Research Centre
RWTH Aachen University, 52056 Aachen, Germany
Ph: +49-241-8027763, Fax: +49-241-8022199
kalim@umic.rwth-aachen.de

***Abstract*—This paper presents a concept to design a compact planar multiharmonic load transformation network (MHLTN) for the realisation of highly efficient dual-band power amplifiers (PAs). The proposed MHLTN consisting of only transmission-lines can precisely achieve impedance terminations at two distinct nonharmonic frequencies including up to three harmonics without switches or tuning elements. High impedance stubs are deliberately inserted at particular sections of the network for the harmonic frequency termination to be controlled. The topology was applied to implement a class-E PA using a GaN High Electron Mobility Transistor (HEMT) in a hybrid design for GSM1810 and LTE2655 operation. The measured impedances of the passive switchless MHLTN for a dual-band class-E load coupling network are in good agreement with simulation results. With a dual-band input matching network, the measurement results have shown 78.4 % and 61.3 % of peak power added efficiency (PAE) with an associated output power of 37.8 dBm and 36.9 dBm in the lower and upper band, respectively.**

***Index Terms*—Class-E, GaN HEMT, dual-band, optimum impedances, output power, power added efficiency (PAE).**

I. Introduction

Recent developments of modern wireless communication systems result in different communication standards and frequencies [1]. In order to increase the degree of integration of RF frontend integrated circuits (ICs), RF equipment is required to operate signals at different communication standards. Some of these standards need to be used concurrently. This demands multiband receivers and transmitters for multistandard communication protocols such that the total size, weight and power consumption of the terminal is reduced. However, the power amplifier (PA) residing in the transmitter unit presents a design challenge as it has high power levels and is, therefore, responsible for a substantial part of the total DC power consumption.

Several approaches have been investigated for multiband transmitter design namely broadband [2]-[3], unit selection [4]-[5] and reconfigurability [6]-[7]. Broadband techniques present a trade-off between bandwidth and efficiency while the unit selection and reconfigurable concepts require the usage of either power switches or electronic tunable elements, *e.g.* varactors or Micro-Electro-Mechanical Switches (MEMSs). These elements require additional control signals to modify the electrical properties of the reconfigurable elements and may introduce distortions.

A multiband approach [8]-[10] provides the capability to operate at different bands without the need of any switch, while the performance of the PA is optimised at the bands of interest. This is possible without any control signals and reduces the number of components in both the input matching and the load transformation network of the PA. Thus, a multiband design leads to flexible mobile communication equipment with a performance comparable to a single-band design. The major challenge in such an approach is to provide the optimum input and output impedances to the device at multiple bands and the corresponding harmonics.

In this paper, a novel architecture to implement a compact planar dual-band MHLTN for the design of a highly efficient PA is presented. The resulting switchless MHLTN is a concurrent dual-band load coupling network. The proposed approach is applied a class-E PA design with a dual-band input matching network. The MHLTN provides concurrently the required impedances at two distinct bands and their harmonics, while the amplifier achieves peak PAE of 78.4 % and 61.3 % with an output power of 37.8 dBm and 36.9 dBm, respectively.

II. Multiharmonic load network based on transmission-lines

A. Single-band multiharmonic load network

The design of a highly efficient PA implies the optimization of the impedances to be presented to the active device's input and output ports both at fundamental and harmonic frequencies [9]. For a real PA design, up to three harmonics are typically considered.

The class-E PA is a promising topology for high efficiency at high frequencies. The class-E operation principle is explained in detail in [11]. The load impedance at the fundamental frequency of a class-E operation is inductive, while all other harmonic load impedances are assumed to be infinite [12].

A widely used distributed-element topology for class-E PA is shown in Fig. 1. This network provides the optimum fundamental impedance and correct impedance terminations up to the third harmonic frequency. Because, it is the starting

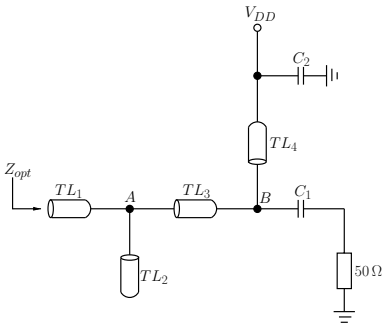

Fig. 1. Schematic of the transmission-line based single-band multiharmonic load transformation network suitable for class-E operation.

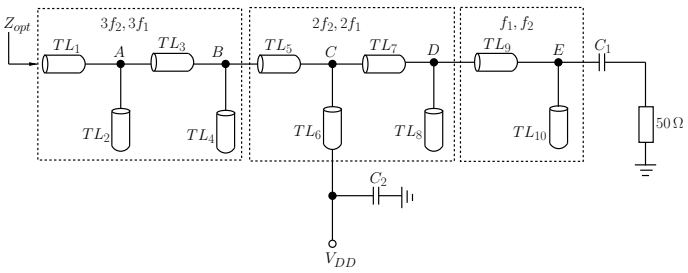

Fig. 2. General schematic for the proposed multiharmonic dual-band load transformation network appropriate for class-E operation.

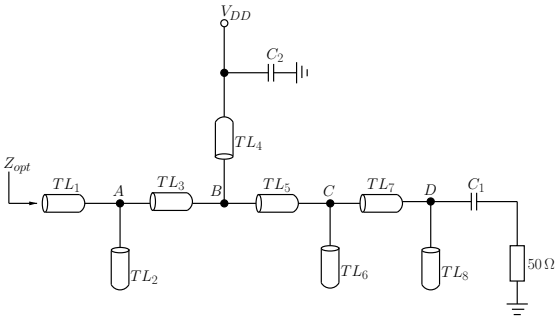

Fig. 3. Schematic of the proposed concurrent dual-band MHLTN for 1.81 GHz and 2.65 GHz class-E load conditions.

point for the proposed dual-band MHLTN, the principle of operation is briefly outlined here. The length of line TL_2 is one quarter wavelength ($\lambda/4$) at $3f_0$, where f_0 is the fundamental frequency. It provides a short circuit at its connection point with TL_1 at node A. Therefore, the circuit to the right of this connection point is ineffective at this frequency. By making TL_1 $\lambda/4$-long at $3f_0$, the low input impedance of TL_2 will be transformed into a high reactive impedance at the transistor's output terminal. Similarly, the impedance at the second harmonic frequency is controlled. TL_4 is made exactly $\lambda/2$-long at $2f_0$ and short-circuited to ground by a large capacitor on one end to provide a low input impedance at node B. The total length of TL_1, TL_3 and the capacitive loading of TL_2 at this frequency are designed to provide a high impedance at $2f_0$ at the output of the transistor. Taking into account the length of TL_1, which is $\lambda/12$, and neglecting the capacitance at this frequency at node A due to TL_2, the electrical length of TL_3 should be approximately $\lambda/24$ at the fundamental frequency f_0. Finally, the required fundamental impedance transformation is obtained by tuning the characteristic impedances of TL_1, TL_2 and TL_3. The capacitor C_1 is used for DC-blocking only and has no effect on the RF performance.

B. Dual-band multiharmonic load network

The proposed dual-band MHLTN uses the concept to insert high impedance stubs of $\lambda/4$ length at specific locations of the network to get a short-circuit for the frequencies to be controlled. The characteristic impedance Z_0 of an open transmission-line and its shunt capacitance are related by:

$$C = \frac{tan(\beta l)}{\omega Z_0}, \tag{1}$$

where β is the propagation constant, l is the length of the line and ω is the angular frequency. According to (1), the high impedance stub has low shunt capacitance which means less capacitive loading and, thus, a marginal influence at the fundamental frequencies. The dual-band MHLTN is designed for class-E conditions, where the lower and upper band frequencies are denoted by f_1 and f_2, respectively.

The concept is implemented by partitioning TL_1 in Fig. 1 into two lines comprising TL_1 and TL_3 as shown in Fig. 2. The high impedance line TL_2 of $\lambda/4$ length at $3f_2$ is used to control the third harmonic of the upper band. It is connected at node A so that TL_1 is $\lambda/4$ at $3f_2$, which provides the required impedance termination at $3f_2$. Similarly, to control the third harmonic of the lower band $3f_1$, the high characteristic impedance line TL_4 of $\lambda/4$ length at $3f_1$ is connected at node B. The length of TL_3 can be tuned according to the capacitive loading of TL_2 and the length of TL_1 in order to obtain the desired impedance termination at this harmonic frequency.

Transmission-line TL_6 of length $\lambda/2$ at $2f_2$ is connected at node C to control the second harmonic of the upper band, $2f_2$. Considering the circuit from the output of the device till node B, TL_5 is tuned to transform the low impedance at node C to the targeted high reactive impedance at the device output at this frequency, while it also provides the required DC-biasing at the drain. To control the second harmonic of the lower band, *i.e.* $2f_1$, TL_8 of $\lambda/4$ length at $2f_1$ is connected at node D. Taking into account the network from TL_1 to node C, TL_7 is adopted to transform the short-circuit at node D to high reactive impedance at the device output.

Finally, the optimum fundamental impedances at the bands of interest are adjusted. For this purpose, transmission-lines TL_9 and TL_{10} along with the characteristic impedances of TL_1, TL_3, TL_5, TL_7 and TL_8 are tuned to obtain optimum load impedances at f_1 and f_2.

III. Concurrent planar dual-band multiharmonic load transformation network design

In this paper, the design has been focused on GSM1810 and LTE2655 bands, *i.e.* 1.81 GHz and 2.65 GHz, respectively.

978-1-61284-757-3/11/$26.00 C2011 IEEE

According to the operating frequencies, $2f_2$ = 5.30 GHz and $3f_1$ = 5.43 GHz. Due to the small frequency spacing between $2f_2$ and $3f_1$, it is difficult to tune them to the desired values. Since, the second harmonics has higher impact on amplifier efficiency, the impedance at $3f_1$ is compromised to achieve the desired impedance at $2f_2$. The high impedance transmission-line TL_4 (illustrated in Fig. 2) is hence removed, while TL_5 can be combined with TL_3 to optimise impedance termination for $2f_2$. The schematic of the proposed concurrent dual-band MHLTN for class-E load conditions is reported in Fig. 3.

IV. Dual-band multiharmonic load transformation network implementation

Based on the single-band multiharmonic load network for class-E PA as discussed in Sec. II, two class-E PAs have been designed at 1.81 GHz and 2.65 GHz, using a large-signal model provided by the manufacturer. A 10 W GaN HEMT from CREE is used for this application. The transistor was biased with a drain supply voltage V_{DD} = 28 V and the gate-to-source bias voltage V_{GS} = -2.6 V. The simulated output impedances along with output power (P_{out}), power added efficiency (PAE) and large-signal gain (G_{LS}) at these two frequencies are summarized in Table I. The concurrent dual-band MHLTN was implemented using the schematic shown in Fig. 3 for the desired impedances. The layout of the design has been analysed and optimised through electromagnetic (EM) simulation using Momentum in Agilent ADS. The dual-band MHLTN was designed and fabricated on Roger RT5870 substrate (ϵ_r = 2.33 and thickness h = 508 μm) whose photo is reported in Fig. 4. The part highlighted by the dotted box controls the harmonic impedances while the remaining part completes the load transformation to the optimum fundamental impedances at the two bands of interest.

TABLE I
Simulated performance of the designed single-band class-E PAs using a GaN HEMT power transistor

f_0 [GHz]	Z_{opt,f_0} [Ω]	$Z_{opt,2f_0}$ [Ω]	$Z_{opt,3f_0}$ [Ω]	P_{out} [dBm]	PAE [%]
1.81	15.7+j23.7	∞	∞	39.7	73.6
2.65	12.5+j13.2	∞	∞	40.8	70.1

The measured output impedances at the fundamental frequencies f_1 and f_2 and the corresponding harmonics are reported in Fig. 5. The fundamental impedances and all higher harmonic impedance terminations are in good agreement with the required impedances (summarised in Table I), except at $3f_1$, which was intentionally compromised for $2f_2$, as discussed in Sec. III.

V. Amplifier Design

The input matching network (IMN) was realised by fulfilling the power matching conditions at the two fundamental frequencies through a dual-band matching network.

Simulated P_{out}, drain efficiency (η) and PAE for an input power of 31 dBm are plotted in Fig. 6, for the frequency range from 1.7 GHz to 2.7 GHz. The simulation of the amplifier results in 75.5 % and 68.0 % PAE with 40.7 dBm and 41.1 dBm output power at 1.81 GHz and 2.65 GHz, respectively. The dual-band performance can be clearly observed at the frequencies of interest with attenuation in between.

The dual-band IMN is then prototyped and the photo of the realised PA is shown in Fig. 7. The total size of the PA module is 5.5 cm x 8.6 cm.

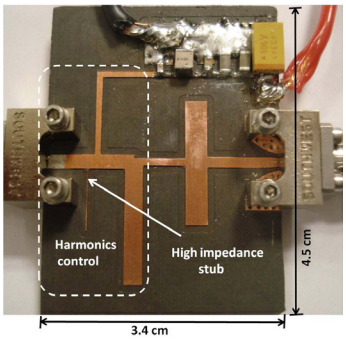

Fig. 4. Photo of the designed dual-band MHLTN of a class-E PA.

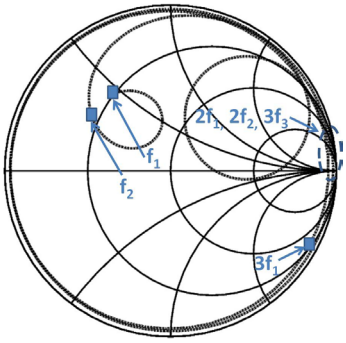

Fig. 5. Measured impedances of the designed concurrent dual-band MHLTN.

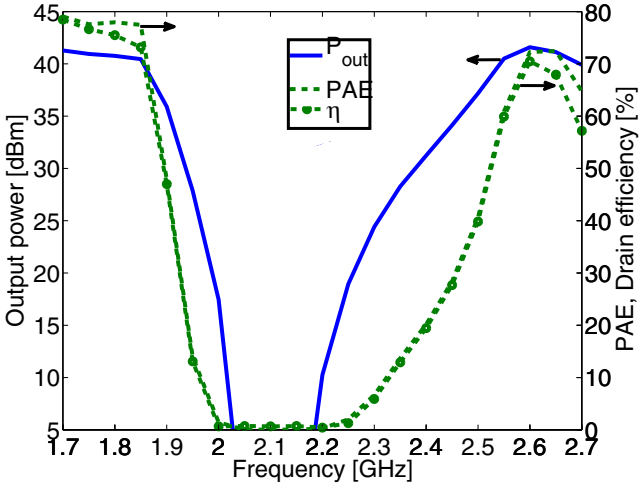

Fig. 6. Simulated drain efficiency, PAE and output power versus frequency of the dual-band class-E PA.

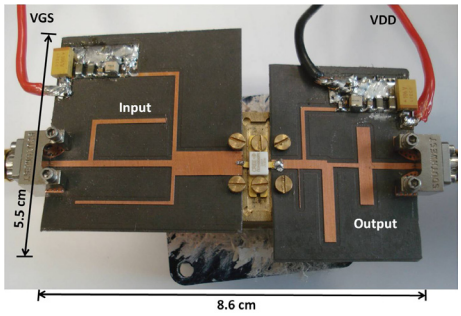

Fig. 7. Photo of the realised class-E PA.

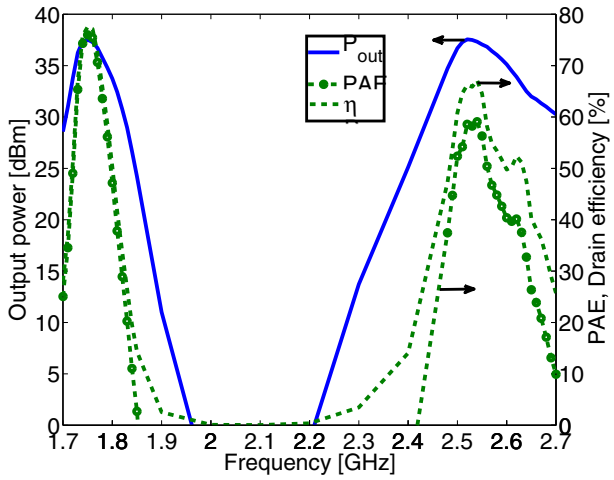

Fig. 8. Measured drain efficiency, PAE and output power versus frequency for $P_{in} = 27.1$ dBm of the dual-band class-E PA.

VI. Measurement Results

A frequency sweep with different input power levels (P_{in}) has been done to measure the performance of the PA in the frequency range form 1.7 GHz to 2.7 GHz. Measured P_{out}, η and PAE of the dual-band PA are plotted in Fig. 8 for $P_{in} = 27.1$ dBm. The two fundamental frequencies are shifted towards the lower frequencies by, respectively, 60 MHz and 110 MHz in the lower and upper bands. This is mainly attributed to inaccuracy of the milling process used to manufacture the microstrip boards. Although there is a frequency variation, the measurement results confirm dual-band performance. Peak PAE of 78,4 % in the low and 61,3 % in the high band has been achieved.

VII. Conclusion

In this work, design, fabrication and measurement of a concurrent dual-band MHLTN using only transmission-lines is presented. The proposed approach is based on a methodology to insert high impedance stubs of $\lambda/4$ length at the particular locations of the network which acts as a short-circuit for the frequencies to be controlled. Secondly, the proper impedance termination due to the high impedance stub marginally affects the MHLTN at the fundamental frequencies because of the low shunt capacitance. This makes the switchless MHLTN easy to design and compact for dual-band applications. The desired and the measured impedances of the passive switchless MHLTN show that the required dual-band impedances for the class-E operation can be precisely synthesised with the proposed approach.

The experimental results of the proposed MHLTN was validated through the fabrication and prototyping of a PA module for 1.81 GHz and 2.65 GHz applications. Measured peak PAE at 1.75 GHz and 2.54 GHz is, respectively, 78,4 % with $P_{out} = 37.8$ dBm and 61.3 % with 36.9 dBm of output power.

Acknowledgment

This work has been supported by cluster of excellence on Ultra high-speed Mobile Information and Communication (UMIC) Research Centre, RWTH Aachen University.

References

[1] M. Steer, "Beyond 3G," *IEEE Microwave Magazine*, vol. 8, no. 1, pp. 76-82, Feb. 2007.

[2] A. Sayed, S. Von der Mark, G. Boeck, "An Ultra Wideband 5W Power Amplifier Using SiC MESFET," *34th European Microwave Conference Proceedings, Amsterdam*, vol. 1, Oct. 2004, pp. 57-60.

[3] C. Mei-Chen, L. Ming-Fong, H. Wang, "A broadband medium power amplifier for millimeter-wave applications," *Asia-Pacific Conference Proceedings, APMC*, vol. 3, Dec. 2005.

[4] S. Zhang, J. Madic, P. Bretchko, J. Mokoro, R. Shumovich, R. McMorrow, "A novel power-amplifier module for quad-band wireless handset applications," *IEEE Trans. on Micrwoave Theory and Tech.*, vol. 51, no. 11, Nov. 2003, pp. 2203-2210.

[5] K. Yamamoto, S. Suzuki, K. Mori, T. Asada, T. Okudo, A. Inoue, "A 3.2-V Operation Single-Chip Dual-Band AlGaAs/GaAs HBT MMIC Power Amplifier with Active Feedback Circuit Technique," *IEEE Journal of Solid State Circuits*, vol. 35, no. 8, Aug. 2000, pp. 1109-1120.

[6] A. Fukuda, H. Okazaki, S. Narahashi, "A Novel Compact Reconfigurable Quad-band Power Amplifier Employing RF-MEMS Switches," *36th European Microwave Conference, Manchester*, Sep. 2006, pp. 344-347.

[7] Q. Dongjiang, R. Molfino, S. M. Lardizabal, B. Pillans, P. M. Asbeck, G. Jerinic, "An intelligently controlled RF power amplifier with a reconfigurable MEMS-Varactor tuner," *IEEE Trans. on Microwave Theory and Tech.*, vol. 53, no. 3, Mar. 2005, pp. 1089-1095.

[8] K. Uchida, Y. Takayama, T. Fujita, K. Maenaka, "Dual-band GaAs FET power amplifier wtih two-frequency matching circuits," *Asia-Pacific Conference Proceedings, APMC*, vol. 1, Dec. 2005, pp. 4-7.

[9] P. Colantonio, F. Giannini, R. Giofre', L. Piazzon, "A Design Technique for Concurrent Dual-Band Harmonic Tuned Power Amplifier," *IEEE Trans. on Micrwoave Theory and Tech.*, vol. 56, no. 11, Nov. 2008, pp. 2545-2555.

[10] R. Negra, A. Sadeve, S. Bensmida, F. M. Ghannouchi, "Concurrent Dual-band Class-F Load Coupling Network for Applications at 1.7 and 2.14 GHz," *IEEE Trans. on Circuits and Systems-II*, vol. 55, no. 3, Mar. 2008, pp. 259-263.

[11] N. Sokal, A. Sokal, "Class E - A new class of high-efficiency tuned single-ended switching power amplifiers," *IEEE Journal of Solid State Circuits*, vol. SSC-10, no. 3, Mar. 1975, pp. 168-176.

[12] T. B. Mader and Z. Popovic, "The transmission-line high efficiency class-E amplifier," *IEEE Microwave Guided Wave Lett.*, vol. 5, no. 9, Sep. 1995, pp. 290-292.